

The Geometric Model for Perceived Roughness Applies to Virtual Textures

Bertram Unger*
Robotics Institute
Carnegie Mellon University

Ralph Hollis†
Robotics Institute
Carnegie Mellon University

Roberta Klatzky‡
Department of Psychology
Carnegie Mellon University

ABSTRACT

A magnetic levitation haptic device (MLHD) is used to simulate a dithered textured surface made up of conical elements. A constraint surface algorithm allows the cone size, shape, mean inter-element spacing and probe size, to be varied in realtime. The high motion bandwidth, fine spatial resolution and high stiffness of the MLHD produce virtual textures with roughness perception characteristics comparable to geometrically similar real textures.

Human subjects use virtual spherical probes of four different sizes to explore textures over a range of element spacings. Roughness magnitude estimates show that roughness initially increases as spacing increases. Maximum roughness is perceived at a spacing governed by the probe-texture geometry. Roughness then decreases as spacing continues to increase. There is an approximately quadratic relationship between texture and spacing. The shape of the magnitude estimation curve, and the texture spacing at which maximum roughness for virtual dithered textures is felt, are similar to those found in real textures having the same geometry. A static geometric model approximately predicts these maxima with consistent underestimation. By incorporating probe velocity into the geometric model, this underestimation can be explained and substantially reduced. Based on these results it is concluded that a haptic device with sufficiently high resolution and bandwidth can be used to accurately generate virtual textures which are perceptually similar in roughness to real textures.

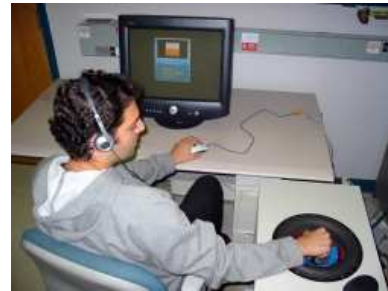
Index Terms: J.4 [Social and Behavioural Sciences]: Psychology—Psychophysics - Haptics;

1 INTRODUCTION

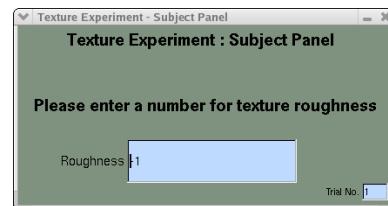
Texture plays a role in object discrimination and provides useful information for examining and manipulating objects, particularly in the absence of vision [9]. Several elements that contribute to the perception of texture include bump size, friction, hardness and stickiness [5]. Of these, roughness perception has received considerable attention but its relationship to the underlying physical properties of texture is still poorly understood. Studies with the bare finger have shown a relationship between surface geometry and roughness magnitude estimates [3, 16] suggesting that finger-pad deformation, as opposed to vibration, is the important determinant of roughness, at least for large element spacings. For smaller spacings, vibrational effects may be significant [4, 6].

When texture is felt via a probe, as when a pen scratches a piece of paper, it seems apparent that vibration must play a role in the texture's perceived roughness. It has been suggested that the interaction between the geometry of the surface and the shape of the probe determines the magnitude of the perceived roughness [10]. Subjects using real spherical probes, exploring a surface of dithered conical elements, perceive roughness to first increase and then decrease as

element spacing increases. The magnitude of the roughness perception is found to be maximum near the point at which the probe can completely penetrate between conical elements.



(a)



(b)

Figure 1: a.) Subject using the magnetic levitation haptic device during psychophysics experiments. b.) Magnitude estimation experiment graphics panel seen by subjects.

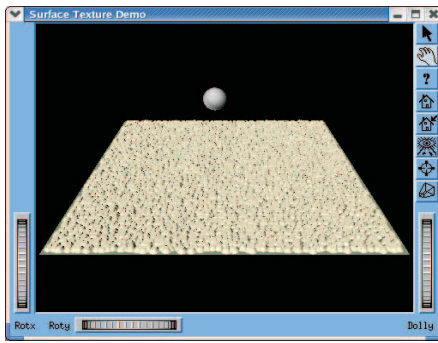
This inverted U-shaped, roughly quadratic psychophysical function is found when subjects explore real dithered surfaces with real three-dimensional probes. A linear function, however, is often found in studies in which subjects explore virtual haptic texture [8, 13, 17, 20]. The surfaces in such studies have commonly been sinusoidal gratings, which subjects encounter using zero-width virtual haptic probes. While it is easy to simulate such a surface and probe, the discrepancy between the psychophysical functions of real dithered surfaces and those of virtual sinusoidal gratings has yet to be explained. It is possible that these differences reflect ways in which the simulation model fails to capture essential details of reality. It is also possible that the haptic hardware is, itself, incapable of rendering some aspect of texture necessary for realistic perception. For example, if vibrational effects are important for roughness perception, the stiffness of the device and its position bandwidth may be inadequate to produce realistic textures.

A logical first step in validating the use of haptic devices for texture simulation would demonstrate that similar virtual and real textures, whose physical parameters closely conform, generate similar psychophysical functions. If the interaction between virtual probe shape and surface geometry is related by the same geometric model that governs real probe-surface interaction, it implies that virtual

*e-mail: bju@andrew.cmu.edu

†e-mail: rhollis@cs.cmu.edu

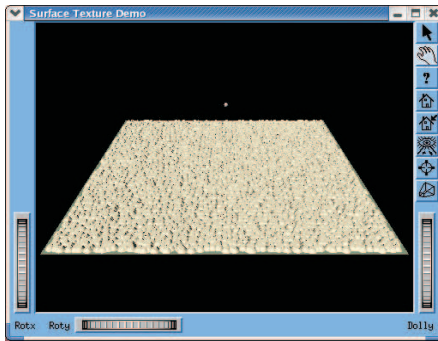
‡e-mail: klatzky@cmu.edu



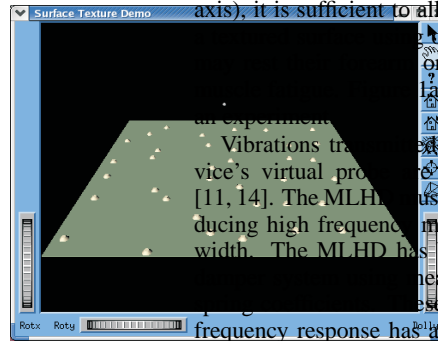
a)



b)



c)



d)

Figure 2: Graphical depiction of the range of constraint surface texture models. Textures have element spacings ranging from 0.5 to 5.5 mm and probe radii ranging from 0.25 to 1.5 mm. a) Probe Size = 1.5 mm, Spacing = 0.5 mm, b) Probe Size = 1.5 mm, Spacing = 5.5 mm, c) Probe Size = 0.25 mm, Spacing = 0.5 mm, d) Probe Size = 0.25 mm, Spacing = 5.5 mm.

textures can be modeled by simulating real texture geometry.

In a previous study by the authors, subjects were asked to explore texture surfaces simulated with a constraint surface algorithm using a magnetic levitation haptic device (MLHD). A just noticeable difference (JND) technique was used to measure subjects' ability to discriminate between different texture spacings when the textures were explored with probes of different sizes. It was found that discriminability thresholds decreased to a minimum as base spacing increased; they then increased again in a way which was readily explainable with reference to a geometric model [19]. These results suggested that the psychophysical function, for a reality-based constraint surface of dithered cones, should be similar to the function found for the originating real texture.

In the study described in the present paper, a magnetic levitation haptic device is used that has high position bandwidth, high stiffness and fine position resolution to generate virtual textures. A constraint surface algorithm is developed which simulates a surface dithered with conical elements whose size, shape and distribution closely reflect studies done with real textures [10]. We hypothesize that minimizing geometric differences between virtual and real textures while using a high fidelity haptic device should result in similar psychophysical functions for roughness magnitude estimation.

2.2 SYSTEM DESIGN

Design

these experiments is a 6-DOF magnetic levitation haptic device [11]. Since the MLHD manipulandum is free-floating, the backlash associated with the actuators and linkages of typical haptic devices are absent. Texture simulation requires rapid trajectory motions which may be limited by the position bandwidths and resolution of typical mechanical-linkage devices. The MLHD has a position resolution of 5-10 μm which allows for the simulation of textures with fine scale. Texture elements may be simulated with accuracies approaching those of standard manufacturing techniques. It also has a maximum stiffness of 25 N/mm in translation and 50 Nm/rad in rotation which is sufficient to render perceptually hard surfaces. While the workspace of the MLHD is small (± 12 mm in translation, $\pm 7^\circ$ rotation about any axis), it is sufficient to allow a user to make a pen-like stroke over the device enclosure, thereby reducing the device to only wrist and fingertip motion. The user shows a subject using the device during an experiment. Vibrations transmitted to the user's hand through a haptic device's virtual probe are thought to affect roughness perception [11, 14]. The MLHD must therefore be capable of accurately reproducing high frequency motion and requires a high position bandwidth. The MLHD has been modeled as a second order spring-mass-damper system. Measurements of the MLHD's damping and stiffness have proven to be highly linear. The modeled frequency response has a ± 3 dB corner at approximately 120 Hz with a slow roll off and significant power up to 1000 Hz. It should therefore be able to simulate texture with vibrational components in the range of both RA and Pacinian neural receptors, both of which may be involved in sensing roughness [7].

2.2 Constraint Surface Texture Modeling

Previous work with real textures by Klatzky *et al* inspired the development of a virtual constraint surface texture model. This model is capable of simulating virtual surface geometries similar to those used in her group's study of the effects of geometry on texture roughness perception. This allows direct comparison of virtual and real psychophysical perception profiles.

The constraint surface model describes the motion of a spherical probe tip across a set of identical, truncated conical elements. As seen in Fig. 3, each cone has a base radius R_{base} , and a top radius R_{top} . The sides of the cone rise with angle α , to a circular plateau. The height of the cone C_h , is determined by these parameters as

$$C_h = (R_{base} - R_{top}) \tan(\alpha). \quad (1)$$

The conical elements are situated on a smooth surface defined by the x, y plane. In order to generate an apparently random spacing distribution while preserving a mean spacing distance between the cones, the elements are first laid out in a regular square grid pattern. Elements are then dithered by some percentage of their initial spacing using zero-mean white noise. Examples of dithered conical element surfaces and spherical probes are shown in Fig. 2.

The path that a spherical probe will take as it passes over a cone is dictated by the geometry of the probe-element interaction. If a probe of radius R_p travels around a convex corner that has greater curvature than the sphere itself, it moves along an arc with radius R_p . Otherwise, it moves a distance R_p from the surface and parallel to it. The probe path is therefore governed by a set of piece-wise continuous functions, with the inflection points between the functions determined by the size of the probe and the shape of the cone. In determining the probe path, it is first necessary to locate the probe with respect to the nearest cone element. The center of the probe is

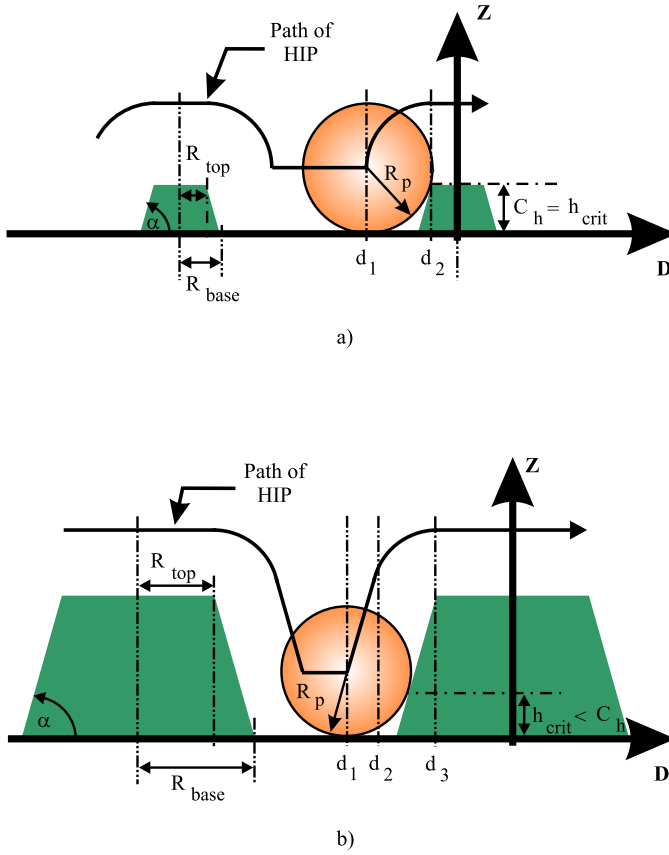


Figure 3: a) Large spherical probe moving over a smaller cone where first contact occurs first at the cone's upper lip. The critical height of contact, h_{crit} , based on the probe radius and angle of the cone, is equal to the cone height, C_h . b) Smaller spherical probe moving over a larger cone where first contact occurs below the cone's upper lip ($h_{crit} < C_h$).

mapped onto the haptic interaction point (HIP). The cartesian distance in the x, y plane, d , is found from the center of the probe to the center of the nearest cone. The nearest cone is found by using the probe's current x, y location as an index into a lookup table which records the dithered position of all cones in their initial undithered rectangular grid. A fast search of this location and its nearest neighbours in the table, quickly determines the closest element. If the probe is farther than d_1 , the point of initial contact, from any cone, the height of the HIP above the surface, z , will simply be that of the probe radius itself. The location of d_1 , and other points of inflection in the probe path, are determined from the probe radius and cone side angle and are defined as distances from the nearest cone element center.

A spherical probe may either make first contact with a cone at its upper edge as shown in Fig. 3a) or at the point along the cone's leading edge where the tangent to the sphere's surface is equal to α as seen in Fig. 3b). The critical height of the first contact, h_{crit} , is found as

$$h_{crit} = R_p(1 - \cos(\alpha)), \quad (2)$$

and is used to divide probe-cone contacts into these two cases. The first case (Fig. 3a), in which $C_h < h_{crit}$ has two probe path inflection points, d_1 and d_2 , which are found as:

$$d_1 = R_{top} + \sqrt{C_h(2R_p - C_h)}, \quad (3)$$

$$d_2 = R_{top}. \quad (4)$$

In this case, the probe's distance, d , from the center of the nearest cone dictates its height z , above the x, y plane as follows:

$$d \geq d_1 : z = R_p, \quad (5)$$

$$d_2 \leq d < d_1 : z = C_h + \sqrt{R_p^2 - (d - R_{top})^2}, \quad (6)$$

$$0 \leq d < d_2 : z = C_h + R_p. \quad (7)$$

The second case, in which $C_h \geq h_{crit}$ (Fig. 3b), has three probe path inflection points

$$d_1 = R_{base} + R_p \sin(\alpha) - h_{crit} \cot(\alpha), \quad (8)$$

$$d_2 = R_{top} + R_p \sin(\alpha), \quad (9)$$

$$d_3 = R_{top}. \quad (10)$$

In this case, the probe's height z , above the x, y plane is determined by d as:

$$d \geq d_1 : z = R_p, \quad (11)$$

$$d_2 \leq d < d_1 : z = \frac{R_p + (R_{base} - d) \sin(\alpha)}{\cos(\alpha)}, \quad (12)$$

$$d_3 \leq d < d_2 : z = C_h + \sqrt{R_p^2 - (d - R_{top})^2}, \quad (13)$$

$$0 \leq d < d_3 : z = C_h + R_p. \quad (14)$$

The calculated heights above the x, y plane are used to constrain the MLHD's motion along the z axis. It is free to move above the constraint surface or along it in x and y .

It should be noted that the probe only ever interacts with a single cone: that which is closest to it. If the spherical probe is in contact with two cones at once, the desired height above the x, y plane is the same as if only one cone were in contact. This occurs because the cones and the probe are symmetric and all cone shapes are identical.

3 EXPERIMENTAL SETUP

The constraint surface algorithm is used to generate a set of textures for evaluation by human test subjects. Textures consist of surfaces of dithered conical elements. Truncated cones with a height, h , of 0.4 mm from the x, y plane are used (see Fig. 3). Their top and bottom radii (R_{top} and R_{base}) are 0.23 mm and 0.52 mm respectively. The top angle, α , is 53.0°. Elements are dithered from a square grid by 40% of the spacing distance. This leaves the mean inter-element spacing unchanged but presents the user with a pseudo-random texture (Fig. 2).

During the experiment, subjects are asked to explore a wide range of texture spacings with spherical probes. Four probe radii of 0.25, 0.50, 1.0 and 1.5 mm are used. Eleven texture spacings are used covering a range of spacings from 0.5 – 5.5 mm. Simulated element shapes, probes sizes and spacing ranges are selected to be as similar as possible to previous studies so that direct comparisons of results with real textures may be made [10].

After receiving IRB approval, fifteen subjects, all of whom indicated they were right-handed, took part in the study. The subjects were drawn from a pool of psychology students who received course credit for participation. Subjects were seated approximately 500 mm from a graphical display and keyboard used to enter roughness magnitude estimates. Textures were presented to the user's right hand by the MLHD manipulandum but no graphical representation of the texture was provided. Users listened to white noise via headphones during the entire experiment to prevent auditory identification of the texture roughness (Fig. 1).

Textures were presented to subjects in four blocks. In each block, subjects explored textures of varying spacing with one of the four probe sizes. The order in which the blocks were presented was randomized to minimize learning effects. Within each block, subjects

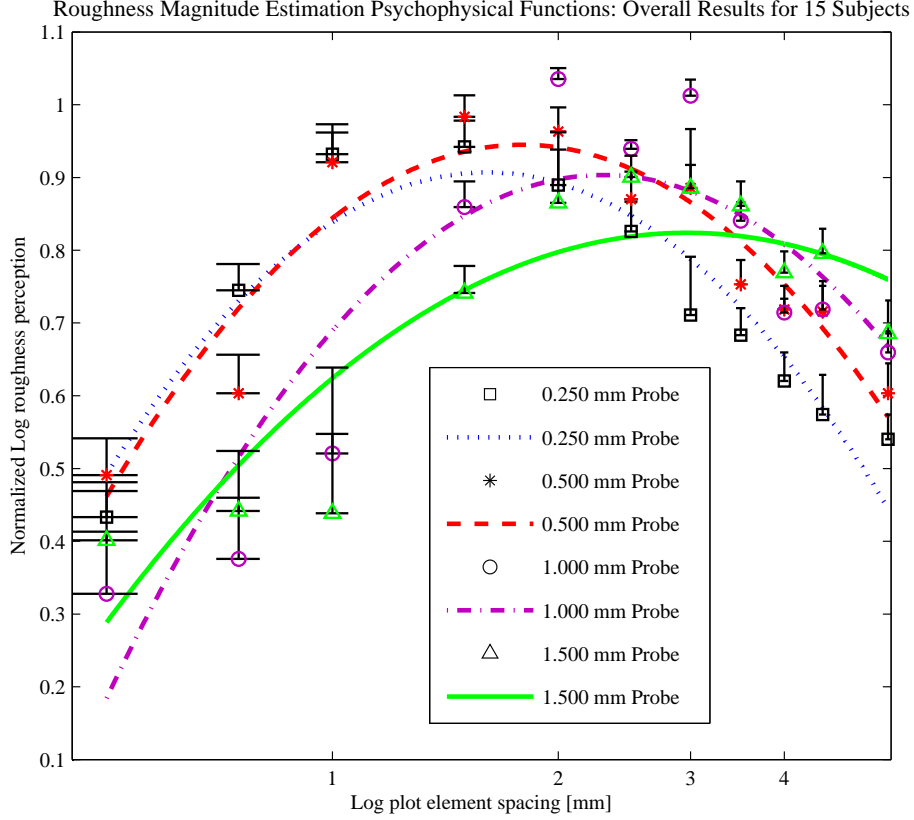


Figure 4: Plot of log magnitude texture roughness versus log spacing (psychophysical function) for four probe sizes. Error bars represent 1 SEM.

experienced 3 repetitions of each of the possible 11 spacings, making a total of 33 trials per block. These 33 trials were presented in random order. Prior to each block of trials, subjects familiarized themselves with a demonstration block of six textures which spanned the range of spacings in the upcoming block. The demonstration blocks used the same probe size as the experiment block which immediately followed it. Demonstration textures were presented in random order of spacing. After completing the demonstration subjects proceeded directly to a block of estimates.

Radius [mm]	a	b	c
0.25	-1.78	0.731	0.828
0.50	-1.86	1.01	0.800
1.00	-1.64	1.19	0.656
1.50	-0.913	0.901	0.588

Table 1: Coefficients of fitted quadratic for roughness estimation data by probe size.

Subjects were allowed to explore any texture for as long as they liked. The experiment had a one hour time limit but all subjects finished well within this time. They were given no instructions on how to explore the texture other than that they were to *feel* it with the provided manipulandum. Subjects were asked to estimate the magnitude of the roughness of each texture and assign it a number. They were told that they could assign textures to any positive range of numbers they wished excluding zero. Low roughnesses were to receive low numbers and high roughnesses were to receive high

numbers. Subjects' roughness estimates were recorded for later analysis. Simultaneous realtime recording of haptic device positions and forces were made at 100 Hz during the experiments.

4 RESULTS

A psychophysical profile of roughness magnitude perception is shown in Figure 4. Each subject repeats 3 trials for each probe size/spacing combination. The mean of these 3 trials is found for each subject, $\bar{X}_{trial}(i, j)$, where i and j indicate probe size and spacing index, respectively. Since there are four probe sizes and 11 spacings, this process results in 44 probe size/spacing values per subject.

Since the scaling of roughness magnitude is left up to individual choice, these values are normalized in order to allow between-subjects comparison. Normalization is performed by finding the mean of a given subject's estimates over all trials, $\bar{X}_{subject}$. The grand mean over all subjects and all trials, $\bar{X}_{experiment}$, is also found. A normalized trial mean for a given subject, \bar{X}_{norm} , is then found as:

$$\bar{X}_{norm}(i, j) = \frac{\bar{X}_{experiment} * \bar{X}_{trial}(i, j)}{\bar{X}_{subject}}. \quad (15)$$

The mean over all n subjects, $\bar{X}_n(i, j)$ for each normalized probe size/spacing combination is then found as:

$$\bar{X}_n(i, j) = \sum_1^n \bar{X}_{norm}(i, j). \quad (16)$$

Probe Radius [mm]	Maximum [mm]	Curvature
0.25	1.61	-1.78
0.50	1.81	-1.86
1.00	2.65	-1.64
1.50	3.15	-0.913

Table 2: Fitted quadratic parameters by probe size.

For each probe size there is now a normalized mean magnitude estimate over all subjects, for each of the eleven possible spacings. These magnitude estimates yield a psychophysical profile for each of the four probe sizes.

The data are presented on a log-log plot as seen in Fig. 4. Psychophysical function profiles frequently display a linear trend on a log-log plot, demonstrating a power fit. Previous studies of texture with the bare finger [16] also demonstrate a power fit for roughness versus spacing and it is therefore convenient to display data in this fashion for comparison with other studies.

The log-log plot of subjects' estimates of texture roughness versus spacing demonstrates an ascending and then descending distribution. This distribution is roughly quadratic, of the form $ax^2 + bx + c$. The coefficients of a quadratic function fitted to the data for each probe size can be seen in Table 1. Quadratic maxima, $-b/2a$, and curvature, a , can be seen in Table 2. The norm of the residuals for a quadratic fit to the data is 0.243 while for a linear fit it is 0.507, when averaged over probe sizes. A one-way analy-

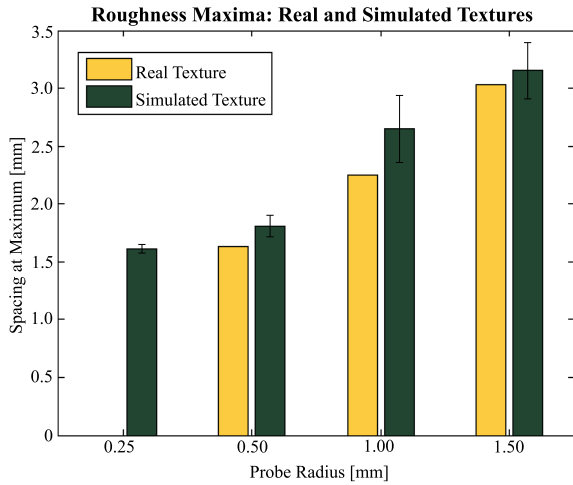


Figure 5: Comparison of real and simulated texture roughness magnitude estimation maxima (DPs). Error bars represent ± 1 SEM. Real texture data is from Klatzky *et al.*'s experiments on size effects with a stylus probe [10]. Real data is unavailable for a probe size of 0.25 mm.

sis of variance (ANOVA) was performed for maxima location and was significant ($p < 1 \times 10^{-6}$), indicating the four probe sizes had significantly different peak locations. A similar ANOVA performed for curvature is also significant ($p < 0.02$) although the trend was not as strong as for the maxima location.

5 DISCUSSION

The quadratic shape of the psychophysical function for roughness versus spacing seen in Fig. 4 has been seen in previous studies of real texture with real probes [10]. Similar studies of roughness psychophysical functions performed with simulated haptic textures have not confirmed these results. This has led to discussion of the

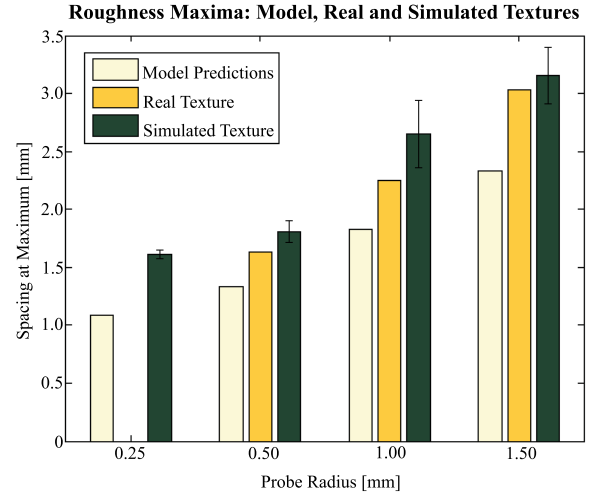


Figure 7: Geometric model predictions of the location of roughness magnitude estimate maxima (DPs) compared with results from real and simulated textures. Error bars represent ± 1 SEM. Real texture data is from Klatzky *et al.*'s experiments on size effects with a stylus probe [10]. Real data is unavailable for a probe size of 0.25 mm.

possibility that the quadratic function is an artifact of the form of analysis used in studies which have demonstrated it (see [13]; but note that the artifact was precluded by analyses in [10]). Typically, such simulated texture studies have been performed using sinusoidal gratings as the texture and a point contact as the probe and they tend to show a linear psychophysical function [8, 13, 17, 20]. Since the underlying texture geometry differs between these simulated haptic studies and those done in reality, it seems logical to conclude that geometric discrepancies account for the differing shape of the psychophysical functions. If this is indeed the case, then a simulated haptic texture which captures essential geometric details of the real texture studies should generate a similar psychophysical function.

In the work presented here, efforts were made to keep texture and probe geometry consistent with previous work [10]. The size and shape of the conical elements and their layout in a dithered pattern, rather than in rows, was considered important. The probes were modeled as spheres and not as points, allowing a representation of probe-texture interaction more in keeping with reality.

As can be seen in Fig. 4, the resulting psychophysical functions clearly show an ascending and descending distribution which can be well-fitted with a quadratic. Examining the location of the maxima of the psychophysical functions seen in Fig. 4, the spacing at which subjects felt maximum roughness, it can be observed that they move to higher spacings as probe size increases. This has been previously noted for real textures [10] and it can be seen from Fig. 5 that the simulated function maxima closely follow Klatzky *et al.*'s real texture findings. Their geometric model of probe and texture interaction provides an explanation for this phenomenon.

In this model, a subject's roughness perception is based on the distance to which the probe penetrates between two elements: the deeper the penetration, the greater the magnitude of perceived roughness. When elements are closely spaced, a spherical probe will not penetrate fully between them as seen in Fig. 6a. When the spacing is large enough the spherical probe drops completely to the floor between elements (Fig. 6b., at the so-called drop point (DP)), and maximum roughness perception occurs. The geometric model predicts that this DP spacing will be at a texture spacing defined by the height, side angle and top radius of the conical elements and the

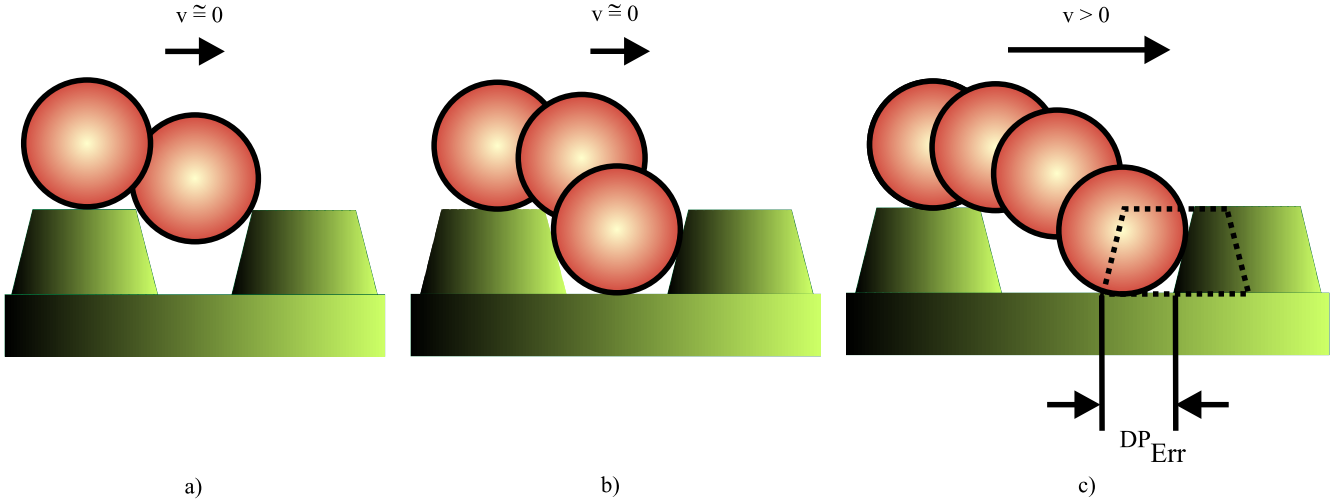


Figure 6: Drop point error explained by probe velocity and geometric model. In a) and b) when velocity is 0, DP is determined only by geometry. In c) with velocity greater than 0, DP is determined by probe velocity and geometry.

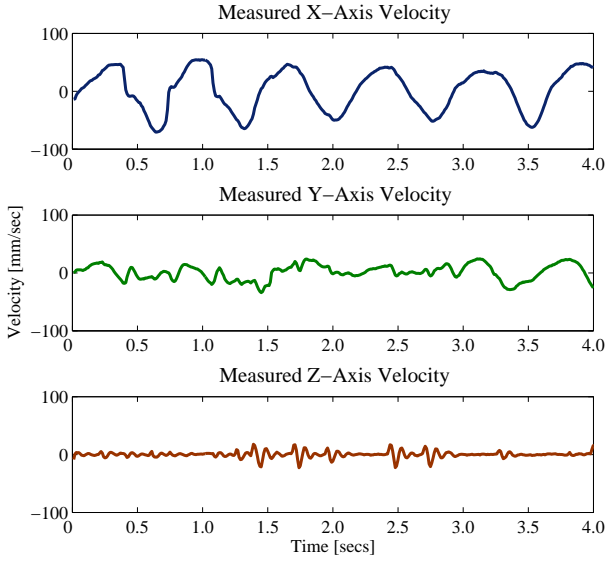


Figure 8: X, Y, and Z-axis probe velocity from position data captured at 100 Hz in realtime during magnitude estimation experiment.

radius of the probe (as defined in Fig. 3) such that

$$DP = R_{top} + \frac{2(h + r(\sin(\alpha)\tan(\alpha) + \cos(\alpha) - 1))}{\tan(\alpha)}. \quad (17)$$

Using eq. 17 it is predicted that as probe size increases the DP will occur at larger and larger spacings. Intuitively, this is because larger probes require larger element spacings before they can fully penetrate between cones. The location of the maxima of the experimentally determined psychophysical functions for four different probe sizes, as well as those the geometric model predicts for the same probe sizes, can be seen in Table 3. Figure 7 demonstrates that the simulation's DPs (as well as real DPs) closely follow the predicted trend, increasing with increasing probe size. Thus the psychological functions for simulated dithered textures match real textures not only in shape, but the location of their maxima can be predicted

Roughness Maxima: Revised Model, Real and Simulated Textures

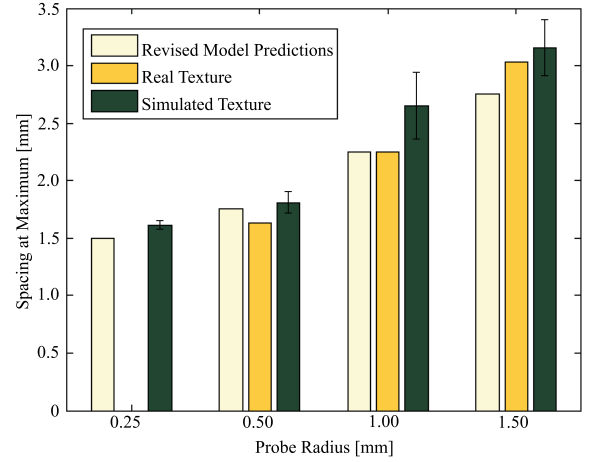


Figure 9: Revised geometric model predictions of the location of roughness magnitude estimate maxima (DPs) compared with results from real and simulated textures. Error bars represent ± 1 SEM. Real texture data is from Klatzky *et al.*'s experiments on size effects with a stylus probe [10]. No real data is available for 0.25 mm probe size.

using the reality-derived geometric model.

Figure 7 also demonstrates that there is consistent underestimation of both real and simulated psychophysical functions by the geometric model. This may be due to the model's underlying quasi-static assumption. The model assumes that the depth of penetration is only related to the position of the probe with respect to texture geometry. The probe actually has some velocity which will carry it forward as it falls to the floor between elements. Element separation must be slightly larger than that predicted by the static model in order for a moving probe to reach the floor without contacting the next element's leading edge as seen in Fig. 6c. A subject's hand and the probe are subject to the force of gravity, F , where

$$F = (M_{hand} + M_{flotor})g. \quad (18)$$

M_{hand} and M_{flotor} are the mass of the hand and flotor respectively

Radius [mm]	Measured Pk [mm]	Predicted Pk [mm]	DP_{err} [mm]
0.25	1.61	1.08	0.530
0.50	1.81	1.33	0.474
1.00	2.65	1.83	0.823
1.50	3.15	2.33	0.822

Table 3: Measured and predicted psychophysical function peak locations and (DP_{err} by probe size).

and g is the acceleration due to gravity. This gravitational force governs the rate at which the probe falls. Thus an approximate idea of the increase in spacing, over and above what the geometric model predicts for the DP, can be calculated from cone height, h and the planar velocity, v_{xy} of the probe. The difference between the velocity-based and quasi-static model predictions for the location of the drop point is termed DP_{err} and is determined as

$$DP_{err} = v_{xy} \sqrt{\frac{2h}{g}}. \quad (19)$$

Mean planar velocity (MPV) over all subjects, trials and probe sizes is determined from 100 Hz position recordings made directly from the haptic device during the experiment. Planar velocity in this experiment is found to vary little between probe sizes and is consistent with velocities used in real texture studies [2, 10, 16]. A representative example of X, Y, and Z-axis realtime probe velocity data can be seen in Fig. 8. Using the measured MPV value of 48.1 mm/sec, a DP_{err} of 0.435 mm was found. This value approaches the average measured DP_{err} of 0.66 mm for the simulated texture and is almost exactly the 0.47 mm DP_{err} found with real textures [10]. When DP_{err} is added to the maxima location predicted by the quasi-static geometric model, as seen in Fig. 9, under-estimation is substantially reduced.

The revised geometric model for roughness perception still consistently underestimates simulated textures by a larger margin than it does for real ones. This may be due to the inherent inability of any haptic device to simulate the very stiff surfaces of real world textures and probes. If the elements in the simulation do not approach infinite stiffness, as they do in reality, the simulated probe will partially penetrate them during collisions. This penetration distance likely is the source of the revised model's small error, as it would tend to further increase the distance a probe travels before reaching the base between elements.

In previous studies, probe velocity has been found to affect the location of maximum roughness, causing it to increase [10, 15]. This is consistent with the predictions of the revised geometric model since higher velocity will result in a larger DP_{err} .

Using a JND technique, it has been found that the sensitivity of roughness perception, as measured by the ability to discriminate between texture spacings, is similar for real and simulated textures [12, 18, 19]. The curvature of the fitted quadratic is another way to approximately measure the sensitivity of roughness perception to changes in spacing. If the roughness of the simulated texture is perceived in the same way as real texture, the curvatures of the psychophysical functions for corresponding probe sizes should be comparable. Figure 10 shows the curvature for probes used in real and simulated textures. The gradual decrease of curvature with increasing probe size indicates that subjects have a harder time discriminating roughness changes with larger probes. This agrees with a previous study by Unger *et al.* in which the threshold of roughness discrimination between spacings increased with probe size [19]. While it is difficult to draw solid conclusions from so few data points, it would seem that the experimental simulated texture created with the constraint surface model, is very close, perceptually, to real texture.

Psychophysical Function Curvatures: Real and Simulated Textures

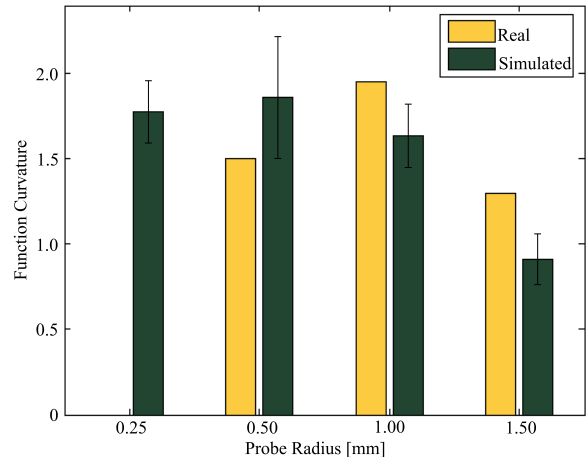


Figure 10: Comparison of real and simulated texture psychophysical function curvature. Error bars represent ± 1 SEM. Real texture data is from Klatzky *et al.*'s experiments on size effects with a stylus probe [10]. No real data is available for 0.25 mm probe size.

The simulated texture curvature slightly underestimates the curvature found with real texture for two of the three probe sizes compared in Fig 10. This implies that, while similar to real textures, the simulated textures are slightly less discriminable. Device effects, resulting from the inability of the MLHD to generate real world stiffnesses and position bandwidths, are the likely cause of this finding.

6 CONCLUSIONS AND FUTURE WORK

6.1 Conclusions

The psychophysical function for roughness perception using a surface of dithered conical elements and a spherical probe is roughly quadratic. This correlates with functions found using similar real surfaces and probes. Moreover, the spacing at which maximum roughness is perceived is found to increase with increasing probe size and is predictable based on a geometric model developed using real probes and textures. By incorporating probe velocity into the geometric model, differences between the model and measured DPs could be accounted for. The comparable psychophysical functions for real and simulated textures demonstrate that a realistic texture roughness can be produced using a haptic device of sufficiently high resolution and bandwidth.

Furthermore, a geometric model of roughness perception appears to predict subjects' perceptions quite well. Differences between the psychophysical function for sinusoidal and dithered texture simulations are likely due to the geometry of the texture and probe and not due to haptic fidelity or flaws in the geometric model. The apparent validity of the geometric model also implies that developing haptic texture models based on texture geometry is a valid and feasible way of designing realistic textures.

6.2 Future Work

Discrepancies exist in the way in which simulations of sinusoidal gratings and dithered textures are perceived [10, 13]. A logical next step would be to determine a geometric model for the interaction of a spherical probe with gratings made up of trapezoidal gratings or sinusoids. In the case of trapezoidal gratings with cross sections similar to the cones used in the present study, the psychophysical function should not differ significantly from dithered textures and, if it does, the discrepancies will need to be examined carefully.

Probe/surface geometry is clearly a significant determinant of roughness perception but other factors, such as compliance, may play a role in how texture is perceived. The development of a psychophysical function for roughness perception using simulations with different stiffnesses could lend insight into how texture is perceived via a probe.

Since the MLHD is capable of accurately recording position and force during exploration of texture simulations, it should be possible to analyze the position and dynamics of the probe/surface interaction in order to better understand the physical properties that are perceived as texture. The relationship of probe dynamics to underlying texture geometry may well be a significant factor in determining texture perception.

Extensions of the model to explain other features of the psychophysical function, such as curvature, might be possible. Concurrent analysis of physical and perceptual data may help determine software and hardware requirements needed to produce realistic virtual textures.

7 ACKNOWLEDGMENTS

This work was supported in part by National Science Foundation grants IRI-9420869 and IIS-9802191.

REFERENCES

- [1] P. J. Berkelman. *Tool-Based Haptic Interaction with Dynamic Physical Simulations using Lorentz Magnetic Levitation*. PhD thesis, Carnegie Mellon University, The Robotics Institute, 1999.
- [2] D. T. Blake, S. Hsiao, and K. O. Johnson. Neural coding mechanisms in tactile pattern recognition: The relative contributions of slowly and rapidly adapting mechanoreceptors to perceived roughness. *The Journal of Neuroscience*, 17(19):7480–7489, 1997.
- [3] C. J. Cascio and K. Sathian. Temporal cues contribute to tactile perception of roughness. *The Journal of Neuroscience*, 21(14):5289–5296, July 2001.
- [4] M. Hollins, S. J. Bensmaia, and S. Washburn. Vibrotactile adaptation impairs discrimination of fine, but not coarse, textures. *Somatosensory and Motor Research*, 18(4):253–262, 2001.
- [5] M. Hollins, F. Lorenz, A. Seeger, and R. Taylor. Factors contributing to the integration of textural qualities: Evidence from virtual surfaces. *Somatosensory and Motor Research*, 22(3):1–14, 2005.
- [6] M. Hollins and S. R. Risner. Evidence for the duplex theory of tactile texture perception. *Perception and Psychophysics*, 62(4):695–705, 2002.
- [7] K. O. Johnson and T. Yoshioka. *Somatosensory System: Deciphering the Brain's Own Body Image*, chapter Neural Mechanisms of Tactile Form and Texture Perception, pages 73–101. CRC, Boca Raton, Florida, 2002.
- [8] R. L. Klatzky and S. Lederman. The perceived roughness of resistive virtual textures: I. Rendering by a force-feedback mouse. *ACM Transactions on Applied Perception*, 3(1):1–14, January 2006.
- [9] R. L. Klatzky, S. Lederman, and C. Reed. Haptic integration of object properties: Texture, hardness, and planar contour. *Journal of Experimental Psychology: Human Perception and Performance*, 15(1):45–47, 1989.
- [10] R. L. Klatzky, S. J. Lederman, C. Hamilton, M. Grindley, and R. H. Swendsen. Feeling textures through a probe: Effects of probe and surface geometry and exploratory factors. *Perception and Psychophysics*, 65(4):613–631, 2003.
- [11] R. L. Klatzky, S. J. Lederman, C. J. Hamilton, and G. Ramsay. Perceiving roughness via a rigid probe: Effects of exploration speed. In *DSC-Vol 67, Proceedings of the ASME Dynamic Systems and Control Division-1999*, pages 27–33, 1999.
- [12] M. Kocsis, H. Z. Tan, and B. D. Adelstein. Discriminability of real and virtual surfaces with triangular gratings. In *Proceedings of the 2007 World Haptics Conference (WHC07): The Second Joint EuroHaptics Conference and Symposium on Haptic Interfaces for Virtual Environment and Teleoperator Systems*, pages 348–353, Tsukuba, Japan, 2007.
- [13] D. Kornbrot, P. Penn, H. Petrie, S. Furner, and A. Hardwick. Roughness perception in haptic virtual reality for sighted and blind people. *Perception and Psychophysics*, 69(4):502–512, 2007.
- [14] L. E. Krueger. David Katz's der aufbau der tastwelt (the world of touch): A synopsis. *Perception and Psychophysics*, 7(6):337–341, 1970.
- [15] S. Lederman and R. Klatzky. Sensing and displaying spatially distributed fingertip force in haptic interfaces for teleoperator and virtual environment systems. *Presence*, 1999.
- [16] S. J. Lederman. Tactile roughness of grooved surfaces: The touching process and effects of macro- and microsurface structure. *Perception and Psychophysics*, 16(2):385–395, 1974.
- [17] P. Penn, D. Kornbrot, S. Furner, A. Hardwick, C. Colwell, and H. Petrie. Roughness perception in haptic virtual reality: the impact of the haptic device, endpoint and visual status. *Unpublished manuscript*, 2004.
- [18] H. Z. Tan, B. D. Adelstein, R. Traylor, M. Kocsis, and E. D. Hirtleman. Discrimination of real and virtual high-definition textured surfaces. In *Symposium on Haptic Interfaces for Virtual Environment and Teleoperator Systems*, pages 3–9, 2006.
- [19] B. Unger, R. Hollis, and R. Klatzky. JND analysis of texture roughness perception using a magnetic levitation haptic device. In *Proceedings of the 2007 World Haptics Conference (WHC07): The Second Joint EuroHaptics Conference and Symposium on Haptic Interfaces for Virtual Environment and Teleoperator Systems*, pages 9–14, Tsukuba, Japan, 2007.
- [20] S. A. Wall and W. S. Harwin. Interaction of visual and haptic information in simulated environments: Texture perception. In *Proceedings of the 1st Workshop on Human Computer Interaction*, pages 39–44, Glasgow, Scotland, 2000.